QUANTUM PROPAGATION IN SINGLE MODE FIBER

Lance G. Joneckis

Laboratory for Physical Sciences
University of Maryland
College Park, MD 20740

Jeffrey H. Shapiro

Department of Electrical Engineering and Computer Science
Massachusetts Institute of Technology
Cambridge, MA 02139-4307

Abstract

This paper presents a theory for quantum light propagation in a single-mode fiber which includes the effects of the Kerr nonlinearity, group-velocity dispersion, and linear loss. The theory reproduces the results of classical self-phase modulation, quantum four-wave mixing, and classical soliton physics, within their respective regions of validity. It demonstrates the crucial role played by the Kerr-effect material time constant, in limiting the quantum phase shifts caused by the broadband zero-point fluctuations that accompany any quantized input field. Operator moment equations—approximated, numerically, via a terminated cumulant expansion—are used to obtain results for homodyne-measurement noise spectra when dispersion is negligible. More complicated forms of these equations can be used to incorporate dispersion into the noise calculations.

1 Introduction

Optical fibers have long been considered for the generation of squeezed-state light, starting with the pioneering work of Levenson and coworkers in the mid 1980's, who observed 0.58 dB of continuous-wave (cw) squeezing [1], to recent measurements exhibiting over 5 dB of short-pulse squeezing [2]. In this paper we present a theory for quantum light propagation in single-mode optical fiber. Our development, which includes the effects of the Kerr nonlinearity, group-velocity dispersion, and linear loss, is guided by two overarching principles: the theory must include all relevant prior results, both classical and quantum mechanical, and, within reasonable limits, it must accommodate arbitrary input states. This theory [3] is an extension of our prior work on quantum propagation in a dispersionless, lossless, Kerr medium [4]. In that earlier study it was shown that a material time constant is crucial to a correct description of quantum nonlinear phase shifts beyond the four-wave mixing regime, a conclusion similar to that reached by Blow and coworkers [5]. The use of a finite Kerr-effect time constant is retained in the current treatment of lossy, dispersive fiber.

This paper is organized as follows. In Section 2 we review quantum propagation in a Kerr medium, concentrating on the structure of the theory and the necessity of a finite Kerr-effect time constant. We recount the principal result of [4], namely the limits on squeezed-state generation

in lossless, dispersionless fiber. Section 3 expands this theory to incorporate dispersion and linear loss via a split-step approach. Section 4 introduces the terminated cumulant expansion (TCE) as a technique for closing the infinite chain of coupled moment equations generated by the full theory. Using the TCE, the limits on quadrature-noise squeezing in lossy, dispersionless fiber are quantified. Finally, in Section 5, we discuss the relationship of our approach to other quantum propagation theories for single-mode fiber, focusing on the necessity of the Kerr-effect time constant.

2   Quantum Self-Phase Modulation

Our attention, in this section, is restricted to a linearly polarized field propagating in a lossless, dispersionless, single-mode fiber that exhibits the Kerr nonlinearity. Classically, the refractive index in this fiber can be written as follows,

$$n(z,t) = n_0 + \frac{n_2 \hbar \omega}{A} |E(z,t)|^2, \tag{1}$$

where z is the axial coordinate along the fiber, t is time, n_0 is the linear refractive index, n_2 is the Kerr coefficient, A is the fiber's effective cross-sectional core area, and $E(z,t)$ is the normalized complex envelope of the single-mode field within the fiber. The field normalization we employ is such that $E(z,t)$ has units $\sqrt{\text{photons/sec}}$. Note that the introduction of the photon energy, $\hbar \omega$, is strictly a convenience at this classical stage; it has no quantum significance as yet.
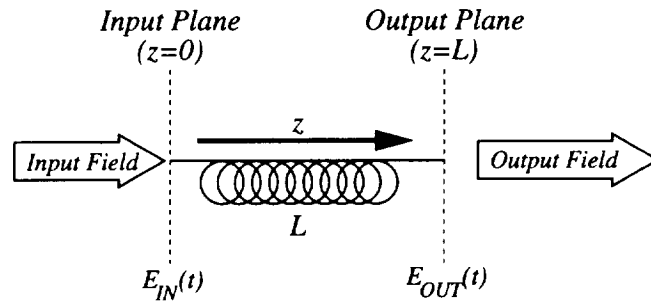

Fig. 1.   Schematic configuration for Kerr-effect propagation in lossless, dispersionless fiber.

The classical propagation problem in lossless, dispersionless, Kerr-effect fiber is sketched in Fig. 1. The fiber is excited, at $z = 0$, by an input field $E_{IN}(t)$ that launches a $+z$-going wave $E(z,t)$ satisfying $E(0,t) = E_{IN}(t)$. In a reference frame moving at the group velocity, v_g, the complex field envelope within the fiber satisfies the following differential equation [6],

$$\frac{\partial E(z,t')}{\partial z} = i\kappa E^*(z,t')E(z,t')E(z,t'), \quad \text{for } z \geq 0, \tag{2}$$

where $t' \equiv t - z/v_g$ is the retarded time,

$$\kappa \equiv \frac{2\pi n_2 \hbar \omega}{A\lambda}, \tag{3}$$

is the nonlinear phase shift per unit length per unit photon flux, and $\lambda = 2\pi c/\omega$ is the center wavelength of the light. The intensity is a constant of motion for Eq. 2, so it is easily shown that

$$E(z,t) = \exp[i\kappa z E^*(0,t')E(0,t')]\, E(0,t'), \quad \text{for } z \geq 0. \tag{4}$$

Using the initial excitation condition that specifies $E(0,t')$, and directing our attention to $E_{OUT}(t) \equiv E(L,t)$, the field coupled out of the fiber at $z = L$, we obtain the classical input-output relation for a length L lossless, dispersionless fiber exhibiting the Kerr nonlinearity, namely,

$$E_{OUT}(t) = \exp[ir E^*_{IN}(t)E_{IN}(t)]\, E_{IN}(t), \tag{5}$$

where

$$r \equiv \kappa L, \tag{6}$$

is the nonlinear phase shift per unit photon flux and, for convenience, we have dropped the L/v_g group delay.

Two well known results follow directly from Eq. 5: spectral broadening through self-phase modulation (SPM), and four-wave mixing (FWM). As an immediate consequence of Eq. 5, we see that an optical pulse propagating through the fiber acquires a time-varying phase shift, which is proportional to the pulse's intensity. The derivative of this time-varying phase constitutes an intensity-dependent instantaneous-frequency variation, implying, for sufficiently intense pulses or long fibers, significant spectral broadening. On the other hand, when the input field comprises a strong monochromatic pump, E^P_{IN}, at frequency ω plus weak sidebands at frequencies $\omega \pm \Omega$, FWM couples the sidebands. The input-output relation for classical FWM can be obtained, from Eq. 5, by replacing the exponential term with its two-term Taylor series approximation, and assuming that all nonlinear phase shifts other than the pump×pump term are small:

$$\tilde{E}_{OUT}(t) = \exp\left(ir|E^P_{IN}|^2\right)\left[(1 + ir|E^P_{IN}|^2)\tilde{E}_{IN}(t) + ir(E^P_{IN})^2\tilde{E}^*_{IN}(t)\right], \tag{7}$$

where $\tilde{E}(t) \equiv E(t) - E^P$ for the input and output fields.

In the quantum theory of the Kerr interaction the photon-units complex field envelope, $E(z,t)$, becomes a photon-units field operator, $\hat{E}(z,t)$. The input field operator—$\hat{E}_{IN}(t) \equiv \hat{E}(0,t)$—is a single-spatial mode, multitemporal-mode free field, and hence must satisfy the following δ-function commutator rule [7],

$$\left[\hat{E}_{IN}(t), \hat{E}^\dagger_{IN}(u)\right] = \delta(t - u), \tag{8}$$

for photon-units field operators. The output field operator—$\hat{E}_{OUT}(t) \equiv \hat{E}(L,t)$—is *also* a single-mode free field, whose commutator must therefore mimic Eq. 8. This requirement is automatically met by quantizing Eq. 2 as follows,

$$\frac{\partial \hat{E}(z,t')}{\partial z} = i\kappa \hat{E}^\dagger(z,t')\hat{E}(z,t')\hat{E}(z,t'), \quad \text{for } z \geq 0. \tag{9}$$

Quantum FWM emerges from Eq. 9, in a manner that ensures commutator preservation, by decomposing the input field operator, $\hat{E}_{IN}(t)$, into a c-number pump, E^P_{IN}, plus a δ-function commutator field operator, $\tilde{\hat{E}}_{IN}(t)$. Then, assuming that all nonlinear phase shifts other than the

pump×pump term are small, Eq. 9 can be linearized and solved to yield the quantum version of Eq. 7, namely,

$$\hat{\bar{E}}_{OUT}(t) = \exp\left(ir|E_{IN}^P|^2\right)\left[(1 + ir|E_{IN}^P|^2)\hat{\bar{E}}_{IN}(t) + ir(E_{IN}^P)^2\hat{\bar{E}}_{IN}^\dagger(t)\right]. \tag{10}$$

Equation 10 is commutator preserving, does not require a Kerr-effect time constant, is consistent with the classical FWM theory, and agrees with experimental results in fiber squeezed-state generation [1].

We find that it is not possible to treat quantum SPM from Eq. 9, in a way that recovers the classical limit, without a modification of the theory. To highlight the failing of instantaneous-interaction quantum SPM, let us calculate the mean output-field for a coherent-state input field [4]. By direct substitution,

$$\hat{E}(z,t) = \exp\left[i\kappa z\hat{E}^\dagger(0,t')\hat{E}(0,t')\right]\hat{E}(0,t'), \quad \text{for } z \geq 0, \tag{11}$$

can be shown to be the solution to Eq. 9, leading to

$$\hat{E}_{OUT}(t) = \exp\left[ir\hat{E}_{IN}^\dagger(t)\hat{E}_{IN}(t)\right]\hat{E}_{IN}(t), \tag{12}$$

as the quantum version of Eq. 5 under an instantaneous Kerr-interaction model. The output mean field,

$$\begin{aligned} \overline{E}_{OUT}(t) &\equiv \langle E_{IN}(t)|\hat{E}_{OUT}(t)|E_{IN}(t)\rangle \\ &= \langle E_{IN}(t)|\exp\left[ir\hat{E}_{IN}^\dagger(t)\hat{E}_{IN}(t)\right]\hat{E}_{IN}(t)|E_{IN}(t)\rangle. \end{aligned} \tag{13}$$

for a coherent-state input field reduces to

$$\overline{E}_{OUT}(t) = \langle E_{IN}(t)|\exp\left[ir\hat{E}_{IN}^\dagger(t)\hat{E}_{IN}(t)\right]|E_{IN}(t)\rangle E_{IN}(t), \tag{14}$$

because a coherent-state input field obeys the eigenfunction relation

$$\hat{E}_{IN}(t)|E_{IN}(t)\rangle = E_{IN}(t)|E_{IN}(t)\rangle, \quad \text{for all } t. \tag{15}$$

For the rest of the calculation we employ a limiting argument,

$$\begin{aligned} \overline{E}_{OUT}(t) &= \lim_{T\to 0}\left(\langle E_{IN}(t)|\exp\left[(ir/T)\int_{t-T}^t d\tau\, \hat{E}_{IN}^\dagger(\tau)\hat{E}_{IN}(\tau)\right]|E_{IN}(t)\rangle\right)E_{IN}(t) \tag{16} \\ &= \lim_{T\to 0}\left(\exp\left[(\exp(ir/T) - 1)\int_{t-T}^t d\tau\, |E_{IN}(\tau)|^2\right]\right)E_{IN}(t) \tag{17} \\ &= E_{IN}(t), \tag{18} \end{aligned}$$

where we have exploited the characteristic function for coherent-state photon counting [8] to obtain Eq. 17.

Equation 18 predicts that the instantaneous Kerr nonlinearity has *no* effect whatsoever on the mean field of a coherent-state input, regardless of how large the classical, peak nonlinear phase shift becomes! This result contradicts the classical theory, Eq. 5, and, more importantly, it contradicts

experiments which have confirmed the classical spectral-broadening predictions. In retrospect, the failure of Eq. 9 to reproduce SPM in the appropriate limit should not be too surprising as it arises from applying an instantaneous, spectral-broadening nonlinearity to a quantized field whose vacuum-state fluctuations extend to infinite bandwidth.

The classical SPM result can be recovered from our quantum mean-field calculation by introducing a phenomenological Kerr-effect time constant, τ_K, as a lower-bound for T in Eq. 16. In particular, with $T = \tau_K > 0$ and $r/\tau_K \ll 1$, Eq. 17 becomes

$$\overline{E}_{OUT}(t) \approx \exp\left[(ir/\tau_K)\int_{t-\tau_K}^{t} d\tau \, |E_{IN}(\tau)|^2\right] E_{IN}(t)$$

$$\approx \exp\left[ir|E_{IN}(t)|^2\right] E_{IN}(t), \tag{19}$$

whenever τ_K is smaller than any classical time scale present in the field.

To incorporate τ_K into our quantum propagation theory for the lossless, dispersionless, Kerr effect in single-mode fiber, we employ the following partial mode expansion for the input-field operator:

$$\hat{E}_{IN}(t) = \sum_{n=-\infty}^{\infty} \hat{a}_n^{IN} \xi(t - n\tau_K), \tag{20}$$

where $\{\, \hat{a}_n^{IN} : -\infty < n < \infty \,\}$ is a set annihilation operators, and

$$\xi(t) \equiv \begin{cases} \dfrac{1}{\sqrt{\tau_K}}, & \text{for } 0 \leq t < \tau_K, \\[2mm] 0, & \text{otherwise,} \end{cases} \tag{21}$$

is a c-number, τ_K-second duration, rectangular pulse. Suppressing the L/v_g-second group delay, the same expansion applies to the output field operator, $\hat{E}_{OUT}(t)$, with the input annihilation operators replaced by the output annihilation operators, $\{\, \hat{a}_n^{OUT} : -\infty < n < \infty \,\}$. These output annihilation operators are related to their corresponding inputs by

$$\hat{a}_n^{OUT} = \exp\left[(ir/\tau_K)\hat{a}_n^{IN\dagger}\hat{a}_n^{IN}\right] \hat{a}_n^{IN}, \quad \text{for } -\infty < n < \infty, \tag{22}$$

which should be compared with the instantaneous quantum Kerr model, Eq. 12.

Equations 20–22 comprise a coarse-grained time model for quantum Kerr-effect propagation in lossless, dispersionless, single-mode fiber. Introducing the Kerr time-constant as a simple phenomenological parameter, τ_K, is arguably a distasteful ad hoc procedure, but the known existence of finite Kerr response times plus the inconsistency of an instantaneous quantum Kerr model mitigate against this deficiency. A more important consideration with respect to Eqs. 20–22 is that they are fundamentally incomplete; $\{\, \xi(t - n\tau_K) : -\infty < n < \infty \,\}$ is an orthonormal temporal mode set, but not a *complete* orthonormal mode set. Hence, in the coarse-grained time model, the input field commutator obeys

$$\left[\hat{E}_{IN}(t), \hat{E}_{IN}^{\dagger}(u)\right] = \delta_{\tau_K}(t, u)$$

$$\equiv \begin{cases} \dfrac{1}{\tau_K}, & \text{if } (n-1)\tau_K \leq t, u < n\tau_K, \text{ for } n \text{ an integer,} \\[2mm] 0, & \text{otherwise.} \end{cases} \tag{23}$$

This expression is *not* the δ-function commutator that a photon-units field operator should possess. However, as will be made clear below, it *can* be a reasonable approximation thereto. Moreover, from Eqs. 22 and 23, we see that the coarse-grained time quantum theory is consistent in that it preserves δ_{τ_K}-function commutators—we have that

$$\left[\hat{E}_{OUT}(t), \hat{E}_{OUT}^\dagger(u)\right] = \delta_{\tau_K}(t, u). \tag{24}$$

Given the approximate nature of the coarse-grained model's field commutator [4], what conditions suffice to ensure the accuracy of this model's moment predictions? Clearly, this model is a poor approximation for field dynamics occurring on time scales comparable to τ_K, or, equivalently, over bandwidths of the order of τ_K^{-1}. We expect τ_K to fall in the interval 1–100 fs—to match the known time scales of n_2—so our quantum input field, $\hat{E}_{IN}(t)$, must *not* have excited (non-vacuum state) modes at these time or bandwidth scales. Furthermore, because SPM causes spectral broadening, we must check that this same time/bandwidth scale condition is satisfied by the *output* field operator, $\hat{E}_{OUT}(t)$. Finally, we must limit any photodetection measurements that we make on the output field to be insensitive to $\hat{E}_{OUT}(t)$-behavior at τ_K time scales or τ_K^{-1} bandwidths. When all three of these conditions apply, we believe the coarse-grained time quantum Kerr model—with a proper value for τ_K—should capture the full behavior of quantum Kerr propagation in lossless, dispersionless, single-mode fiber.

The output mean-field derivation—with a Kerr time-constant τ_K—is virtually identical to the analysis of the instantaneous-interaction case. We find that

$$\overline{E}_{OUT}(t) \equiv \langle E_{IN}(t)|\hat{E}_{OUT}(t)|E_{IN}(t)\rangle = \exp\left[iR|E_{IN}(t)|^2\right] E_{IN}(t), \tag{25}$$

where we have defined the complex number, R, according to

$$iR \equiv [\exp(i\phi_q) - 1]\tau_K, \quad \text{for } \phi_q \equiv r/\tau_K. \tag{26}$$

Equation 25 bears a striking similarity to the classical formula, Eq. 5. Indeed, the two would be identical were $R = r$ to prevail.

We know that r is the *classical* nonlinear phase shift per unit photon flux. Because τ_K is the time duration of a single, rectangular-pulse mode in our coarse-grained time model, we have that ϕ_q is *numerically* the classical phase shift produced by one photon in such a mode. Equation 25 applies to a coherent-state input field—which has vacuum-fluctuation noise in *all* its modes—so it is fair to regard ϕ_q, *physically*, as the quantum nonlinear phase shift that is due to the vacuum fluctuations of a single mode.

The predictions of the quantum and classical theories are nearly coincident when we have $r \approx \text{Re}(R)$ and $|\text{Im}(R)| \ll 1$. These conditions hold for $\phi_q \ll 1$, as can be seen from Fig. 2, where we have plotted $\text{Re}(R)/r$ and $\text{Im}(R)/r$ vs. ϕ_q. Assuming $\tau_K = 1$ fs, a 1 km fused silica fiber will have $\phi_q \approx 10^{-3}$ rad; from Fig. 2 we conclude that Eq. 25, the quantum coherent-state mean field, will then be in excellent agreement with Eq. 5, the classical mean field result. For $\phi_q > 10^{-1}$ rad, there is a pronounced divergence between $\text{Re}(R)$ and r, caused by the intrinsic periodicity of R. Viewed as a function of ϕ_q, Eq. 26 shows that R is periodic with period 2π. Physically, this periodicity constitutes a quantum state-recurrence for Kerr-effect propagation in lossless, dispersionless fiber and occurs when $L = L_q \equiv 2\pi\tau_K/\kappa$; for $\tau_K = 1$ fs and fused-silica

fiber this implies $L_q \sim 10^4$ km, an experimentally inaccessible value for our assumptions of zero loss and zero dispersion.
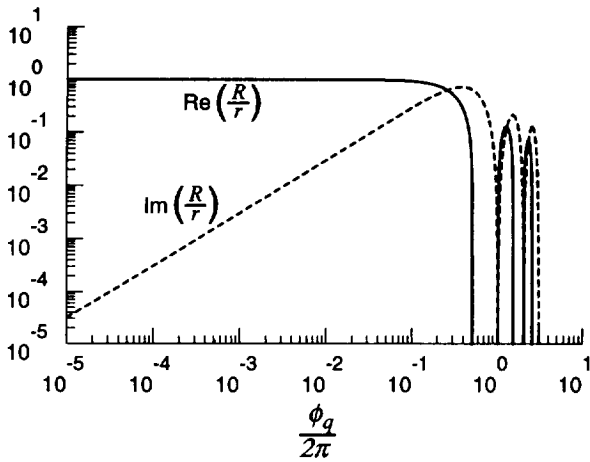

Fig. 2. Logarithmic plots of Re(R)/r and Im(R)/r vs. ϕ_q. The coherent-state mean field of coarse-grained time SPM reduces to the classical SPM result when R $\approx$ r; ϕ_q is the quantum nonlinear phase shift, i.e., the Kerr-induced phase shift of one photon per τ_K-second mode.
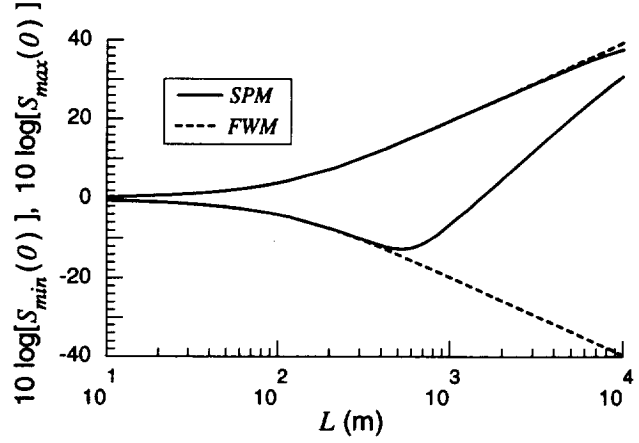
Fig. 3. Minimum and maximum low-frequency, homodyne-measurement noise spectra for a cw, coherent-state input vs. fiber length. The solid curves are the coarse-grained time SPM theory; the dashed curves are the instantaneous-interaction FWM theory. The parameter values employed are: $\lambda = 1.06\,\mu$m; A $= 3.56 \times 10^{-11}\,\mathrm{m}^2$; $n_2 = 3.2 \times 10^{-20}\,\mathrm{m}^2/\mathrm{W}$; $P_{IN} = 1$ W; and $\tau_K = 1$ fs.

Expressions for the quantum output moments, up to the second order, have been derived for Gaussian-state inputs [4]. We note that these moments yield the correct results in the appropriate limits. Specifically, when $\phi_q \ll 1$ they are in agreement with the quantum FWM results. Furthermore, if we let $R \longrightarrow r$ and $\delta_{\tau_K}(t, u) \longrightarrow 0$ and use classical covariances in lieu of quantum covariances throughout, e.g., $\langle \hat{E}_{IN}^\dagger(t)\hat{E}_{IN}(u)\rangle \longrightarrow \overline{E_{IN}^*(t)E_{IN}(u)}$, etc., the resulting equations agree with classical stochastic SPM results. We note that *none* of these classical formulas depend on the Kerr-effect time constant, τ_K. This is fully consistent with our assumption that the spectrum of the classical input excitation *and* the implied output-field spectrum are both narrower than τ_K^{-1}. Under these circumstances we expect—in a classical theory—that the Kerr interaction is effectively instantaneous.

The implications of the full theory are readily ascertained by examining the output field's homodyne-detection statistics. An ideal homodyne measurement on $\hat{E}_{OUT}(t)$ yields a photocurrent whose statistics are proportional to those of the following abstract quantum measurement:

$$\hat{E}_\phi(t) \equiv \hat{E}_{OUT}(t)e^{i\phi} + \hat{E}_{OUT}^\dagger(t)e^{-i\phi}, \tag{27}$$

where ϕ is the local-oscillator (LO) phase. As is conventionally done in cw squeezing experiments, we shall focus on the minimum and maximum values of the homodyne-noise spectra as the LO phase is varied.

457

For a coherent-state input, both the instantaneous-interaction FWM and the coarse-grained time SPM theories imply frequency-independent homodyne spectra out to frequencies comparable to τ_K^{-1}. In Fig. 3 we have plotted $S_{min}(0)$ and $S_{max}(0)$, vs. fiber length L, for both theories. These curves assume $n_2 = 3.2 \times 10^{-20} \, \mathrm{m^2/W}$, $A = 3.56 \times 10^{-11} \, \mathrm{m^2}$, $\lambda = 1.06 \, \mu\mathrm{m}$, $P_{IN} \equiv \hbar\omega |E_{IN}|^2 = 1 \, \mathrm{W}$, and, for the coarse-grained time case, $\tau_K = 1 \, \mathrm{fs}$. Quantum FWM predicts complete noise suppression for one quadrature component, $S_{min}(0) \longrightarrow 0$, as the fiber length becomes infinite. Moreover, this transpires at minimum uncertainty product, $S_{min}(0)S_{max}(0) = 1$. These FWM features are clearly evident is Fig. 3; for long enough fibers, however, they are at odds with our coarse-grained time SPM theory. According to Fig. 3, the coarse-grained time SPM theory has an $S_{min}(0)$ which reaches a *nonzero* minimum at $L \approx 500 \, \mathrm{m}$, and increases, for longer fibers, substantially above the coherent-state value of unity.

The precise location of the minimum in the low noise quadrature depends on τ_K with higher values of τ_K extending the region of agreement between the instantaneous interaction FWM and the coarse-grained time SPM theories. For various technical reasons, e.g., guided acoustic-wave Brillouin scatter, it is not feasible to perform such an experiment using a cw field. Nevertheless, the physical conditions corresponding to the minimum in Fig. 3, namely 1 Watt input power and roughly a 500-meter-long fiber, seem well within the realm of possibility for pulsed experiments. In fact, modeling Shelby's soliton-squeezing experiments [9] by using his peak intensity as the intensity in our cw theory, we find that conditions are right for a τ_K-dependent deviation from quantum FWM. However, accurate analysis of a short-pulse experiment—especially one based on solitons—must surely account for group-velocity dispersion. In addition, a realistic quantum propagation theory for long fibers should address linear loss.

3 Inclusion of Dispersion and Loss

A split-step configuration for incorporating group-velocity dispersion (GVD) and linear loss (LL) into quantum propagation analysis for a Kerr-nonlinear fiber is shown schematically in Fig. 4. An infinitesimal length of fiber at z is divided into two sub-segments. The first sub-segment exhibits only the Kerr nonlinearity and linear loss; the second has neither Kerr effect nor loss, but suffers from dispersion.

Let $\hat{E}(z,t)$ be the coarse-grained time, $+z$-going, photon-units field operator within the fiber, i.e., as before we have the mode expansion

$$\hat{E}(z,t) = \sum_{n=-\infty}^{\infty} \hat{a}_n(z)\xi(t - n\tau_K). \tag{28}$$

Over an infinitesimal, δz-meter-long fiber segment, the split-step procedure leads to the z-to-$(z + \delta z)$ annihilation operator transformation,

$$\hat{a}_n(z + \delta z) = \sum_{m=-\infty}^{\infty} h[n - m; \delta z]\hat{\tilde{a}}_m(z), \quad \text{for } -\infty < n < \infty, \tag{29}$$

where

$$\hat{\tilde{a}}_n(z) \equiv \exp\left[i(\kappa\delta z/\tau_K)\hat{a}_n^\dagger(z)\hat{a}_n(z) + (\alpha/2)\delta z\right]\hat{a}_n(z) + \sqrt{\alpha}\delta z\hat{b}_n(z), \quad \text{for } -\infty < n < \infty, \tag{30}$$

characterizes SPM and LL *alone* over the dispersionless sub-segment, and

$$h[n; \delta z] \equiv \begin{cases} -\dfrac{i\beta_2}{2\tau_K^2}\delta z, & \text{for } n = -1, 1, \\[2mm] 1 + \dfrac{i\beta_2}{\tau_K^2}\delta z, & \text{for } n = 0, \\[2mm] 0, & \text{otherwise,} \end{cases} \tag{31}$$

is a discrete-time impulse response accounting for the dispersive sub-segment. In Eqs. 28–31, we have suppressed the group-velocity delay, and we have introduced the fiber's dispersion coefficient, β_2, and its power-attenuation coefficient, α. More importantly, with the inclusion of a Langevin noise-operator $\hat{b}_n(z)$ required by the presence of the LL these equations preserve the $\delta_{\tau_K}(t, u)$-function commutator of a coarse-grained time input field operator, $\hat{E}_{IN}(t)$. So, if we drive the fiber at $z = 0$ with such an input—forcing $\hat{E}(0, t) = \hat{E}_{IN}(t)$—and then iteratively apply Eqs. 28–31, we will arrive at an output field operator, $\hat{E}_{OUT}(t) \equiv \hat{E}(L, t)$ at $z = L$ with a proper coarse-grained time commutator. Furthermore, because the unitary operators that transform the $\{\hat{a}_n(z)\}$ into the $\{\hat{\bar{a}}_n(z)\}$ are known, as are the operators for changing the $\{\hat{\bar{a}}_n(z)\}$ into the $\{\hat{a}_n(z + \delta z)\}$, we can—in principle—calculate *all* the measurement statistics for $\hat{E}_{OUT}(t)$, given any state of $\hat{E}_{IN}(t)$.
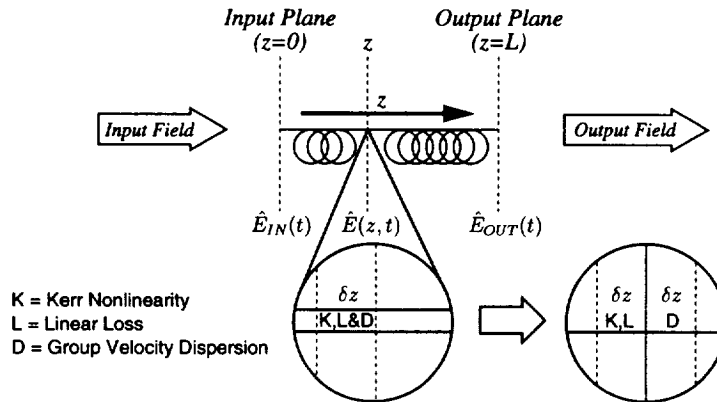

Fig. 4. Schematic split-step configuration for inclusion of group-velocity dispersion and linear loss into the coarse-grained time SPM theory.

We note that the only aspect missed in this split-step approach is a term proportional to the commutator of the Hamiltonians governing each step. It can be shown that this commutator is finite and its contribution goes to zero in δz^2; hence, in the limit of $\delta z \longrightarrow 0$ this is an exact theory. Taking the limit of $\delta z \longrightarrow 0$, the differential equation for the mode operator is

$$\frac{\partial}{\partial z}\hat{a}_n(z) = -(\alpha/2)\hat{a}_n(z) + i(\kappa/\tau_K)\hat{a}_n^\dagger(z)\hat{a}_n^2(z) + \frac{i\beta_2}{2\tau_K^2}[2\hat{a}_n(z) - \hat{a}_{n-1}(z) - \hat{a}_{n+1}(z)]$$

$$+ \sqrt{\alpha}\hat{b}_n(z), \quad \text{for } 0 \le z \le L, \ -\infty < n < \infty. \tag{32}$$

The coarse-grained time *cannot* be suppressed—it is essential to preventing the mean-field contradiction exhibited in Sect. 3.1—but it can be hidden. Returning to field operator notation, Eq. 32

can be recast as

$$\frac{\partial}{\partial z}\hat{E}(z,t) = i\kappa\hat{E}^\dagger(z,t)\hat{E}(z,t)\hat{E}(z,t) - i\frac{\beta_2}{2}\frac{\partial^2_{\tau_K}}{\partial_{\tau_K}t^2}\hat{E}(z,t) - \frac{\alpha}{2}\hat{E}(z,t) + \sqrt{\alpha}\hat{F}(z,t) \qquad (33)$$

with the obvious, implied definitions for the τ_K-approximation to the second partial derivative with respect to time and for the Langevin noise field-operator.

Equation 33 is extraordinarily appealing. Converting it, naïvely, to continuous-time classical form by merely dispensing with the operator carets, dropping the Langevin noise source, and the τ_K subscripts, we obtain

$$\frac{\partial}{\partial z}E(z,t) = i\kappa E^*(z,t)E(z,t)E(z,t) - i\frac{\beta_2}{2}\frac{\partial^2}{\partial t^2}E(z,t) - \frac{\alpha}{2}E(z,t), \qquad (34)$$

the well-known starting point for the classical theory of solitons in fiber [6].

4 Moment Propagation and the Terminated Cumulant Expansion

Although it is possible to calculate the exact state transformation for the preceding quantum theory, it is a daunting numerical task in almost all cases of interest. Thus, we have elected to follow a much simpler and restrictive course—moment propagation. Taking the expectation value of Eq. 33 we find that the mean field develops according to

$$\frac{\partial}{\partial z}\langle\hat{E}(z,t)\rangle = i\kappa\langle\hat{E}^\dagger(z,t)\hat{E}(z,t)\hat{E}(z,t)\rangle - i\frac{\beta_2}{2}\frac{\partial^2_{\tau_K}}{\partial_{\tau_K}t^2}\langle\hat{E}(z,t)\rangle - \frac{\alpha}{2}\langle\hat{E}(z,t)\rangle, \qquad (35)$$

which illustrates the fundamental problem of moment propagation—the Kerr nonlinearity couples each moment's differential equation to those of higher order. For example, in the single time case, the differential equation for the moment $\langle\hat{E}^{\dagger k}(t,z)\hat{E}^l(t,z)\rangle$ includes terms containing the moment $\langle\hat{E}^{\dagger k+1}(t,z)\hat{E}^{l+1}(t,z)\rangle$, leading to an infinite progression of coupled differential equations.

This infinite linkage of moment equations can be broken, in an approximate way, through a terminated cumulant expansion (TCE). (A brief review of cumulants—for classical random variables—is found in the Appendix. Here, we rely on normally-ordered quantum cumulants.) In the TCE-K expansion, all normally-ordered quantum-field cumulants beyond the K-th order are set to zero:

$$\left\langle\left\langle\prod_k[\hat{E}^\dagger(z,t)]^{m_k}\prod_k[\hat{E}(z,t)]^{n_k}\right\rangle\right\rangle = 0, \quad \text{when } \sum_k(m_k+n_k) > K. \qquad (36)$$

The TCE-K assumption provides low-order moment expressions for all field-operator moments beyond K-th order. For example, the third-order cumulant relation,

$$\begin{aligned}\langle\langle\hat{E}^\dagger(z,t)\hat{E}^2(z,t)\rangle\rangle &= \langle\hat{E}^\dagger(z,t)\hat{E}^2(z,t)\rangle - 2\langle\hat{E}^\dagger(z,t)\hat{E}(z,t)\rangle\langle\hat{E}(z,t)\rangle \\ &\quad - \langle\hat{E}^\dagger(z,t)\rangle\langle\hat{E}^2(z,t)\rangle + 2\langle\hat{E}^\dagger(z,t)\rangle\langle\hat{E}(z,t)\rangle^2,\end{aligned} \qquad (37)$$

affords the following explicit expression for the TCE-2 expansion:

$$\langle\hat{E}^\dagger(z,t)\hat{E}^2(z,t)\rangle = \langle\hat{E}^\dagger(z,t)\rangle\langle\hat{E}^2(z,t)\rangle + 2\langle\hat{E}^\dagger(z,t)\hat{E}(z,t)\rangle\langle\hat{E}(z,t)\rangle - 2\langle\hat{E}^\dagger(z,t)\rangle\langle\hat{E}^\dagger(z,t)\rangle^2. \qquad (38)$$

Substitution of this expression into the mean-field equation, Eq. 35, eliminates the third-order moment and leads, ultimately, to a closed system of differential equations for

$$\{\langle \hat{E}(z,t)\rangle, \langle \hat{E}^{\dagger}(z,t)\hat{E}(z,u)\rangle, \langle \hat{E}(z,t)\hat{E}(z,u)\rangle\}. \tag{39}$$

The accuracy of the TCE approximation depends upon both the initial state and its subsequent propagation. For a Gaussian state, such as a coherent state, all cumulants of order three or higher vanish. Moreover, a Gaussian state remains Gaussian under linear propagation—even if it is lossy and/or dispersive—so, for example, TCE-2 is *exact* for Gaussian-state inputs in the four-wave mixing limit. Higher-order TCE approximations track deviations from a Gaussian state, hence they should prove useful for Gaussian-state inputs even *beyond* the four-wave mixing regime. This is demonstrated, quantitatively, in Fig. 5, where we compare coherent-state input, homodyne-noise output spectra for a lossless, dispersionless Kerr-effect fiber computed via TCE-K, with the exact solution presented in the previous section. The coarse-grained time SPM curve (exact solution) represents a state that is very nearly Gaussian state up to the point of its minimum-noise curve departs from the instantaneous-interaction FWM curve. (As noted above, coherent-state FWM is always a Gaussian-state case.) The TCE-2 approximation misses the mark, as it always represents a minimum-uncertainty Gaussian state, which is plainly a bad approximation to the exact solution. However, the TCE-3 approximation captures the essential nature of the exact solution, viz. it correctly predicts the minimum noise level and its subsequent rise to the shot-noise-level. As expected, the TCE-4 and TCE-5 approximations show slightly better performance, but the meager improvement they provide hardly justifies their added computational burden.
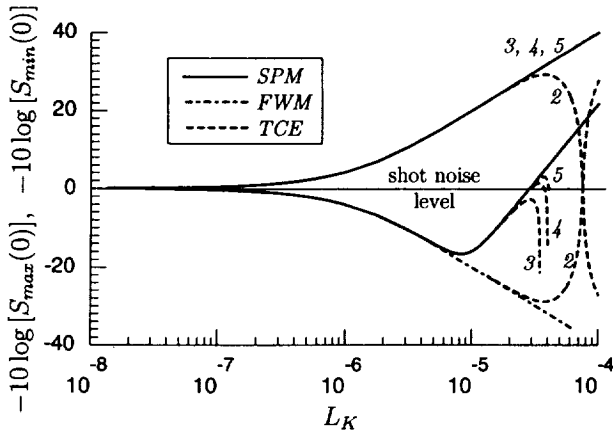

Fig. 5. Minimum and maximum low-frequency, homodyne-measurement noise spectra vs. $_q/2$ ($_q$ = 2 for a fiber of length 3.25 × 10^5 km, $_k$ = 1fs) at 1.55 μm in a dispersionless, lossless fiber. SPM denotes the exact calculation, FWM the four-wave mixing approximation, and TCE the terminated cumulant expansion (K = 2,3,4,5 shown). The input field is a 1-Watt, coherent state; 0 dB is the coherent-state noise level.

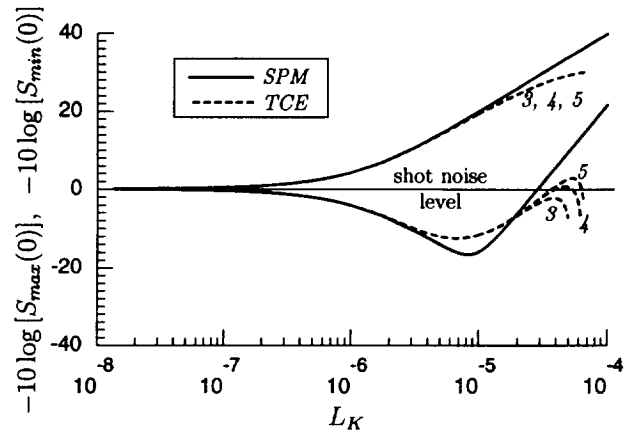Fig. 6. Minimum and maximum low-frequency, homodyne-measurement noise spectra vs. $_q/2$ ($_q$ = 2 for a fiber of length 3.25 × 10^5 km, $_k$ = 1fs) at 1.55 μm in a dispersionless fiber. SPM denotes the exact, lossless calculation, and TCE the terminated cumulant expansion (K = 3,4,5 shown) with 0.2dB/km linear loss. The input field is a 1-Watt, coherent state; 0 dB is the coherent-state noise level.

Armed with the TCE approximation, we can obtain homodyne-noise spectra for situations in which the exact calculations are thwarted by moment linkage. Consider propagation in a lossy,

dispersionless Kerr-effect fiber. In Fig. 6 we have plotted the exact SPM result for the *lossless* case (solid curve) and the TCE solutions (dashed curves) for a fiber with a power loss coefficient of 0.2 dB/km. The regions of overlap follow the same trends seen in Fig. 4, and predict a 4 dB increase in the noise level over the lossless case.

Inclusion of dispersion couples time slots and greatly increases the complexity of TCE moment calculations, even with a coherent-state input. If we address N time samples of the field, there are $(19N + 15N^2 + 2N^3)/3$ complex moments, or $(35N + 30N^2 + 4N^3)/3$ real quantities, to track. Each real quantity obeys one of 23 types of differential equation, which contain anywhere from 5 to 87 terms. For $N = 100$, there are thus 717,300 moments, or 1,434,500 real quantities, to be computed. We are working on these calculations at present, and expect to be reporting our results in the near future.

5 Conclusions

We have presented a general theory for quantum propagation of an optical field in a lossy, dispersive Kerr-effect fiber. Our approach leads to equations that are continuous in space, but discrete in time. The time granularity is set by a phenomenological Kerr-effect time constant needed to properly recover the known results of classical self-phase modulation. Other theories have been developed that describe propagation in such a fiber [11],[16], but ours is the first for which a material time constant has been specifically employed to temper the instantaneous interaction. It has been argued that the presence of dispersion provides a much more constrictive bandwidth limitation than τ_K^{-1}, thereby eliminating the need for this Kerr-effect time constant [17]. We disagree, but in the interests of brevity, we shall confine our remarks to a few brief points. First, it has been shown that there is a four-wave mixing region in which dispersion enhances squeezing [18]; here we may expect that dispersion exacerbates the need for a finite τ_K to correctly determine the validity limit of FWM. On the other hand, if there are propagation regimes—such as soliton propagation—wherein dispersion renders a finite Kerr-effect time constant unnecessary, then that impotence should appear in our calculations, i.e., our noise results should be insensitive to the value we assign to τ_K. Note that, even with loss and dispersion, the value of τ_K is irrelevant to linearized noise analysis, and this includes the linearized noise theory of quantum solitons. Finally, the theory we have presented handles the case of an arbitrary field, in either the normal or anomalous dispersion regimes, and is more encompassing than those restricted to soliton propagation.

Appendix

For a real-valued classical random vector $\vec{X} \equiv (X_1, X_2, \ldots, X_n)$ whose joint characteristic function is $\phi(\vec{s}) \equiv \langle \exp(i\vec{s} \cdot \vec{X}) \rangle$, the cumulants are defined by:

$$\langle\langle \prod_k X_k^{m_k} \rangle\rangle = \left[\prod_k \left(-i\frac{\partial}{\partial s_k} \right)^{m_k} \Phi(\vec{s}) \right]_{\vec{s}=\vec{0}}, \tag{40}$$

where the cumulant generating function is $\Phi(\vec{s}) \equiv \ln(\phi(\vec{s}))$. Higher order cumulants contain information of decreasing significance [10].

References

[1] R.M. Shelby, M.D. Levenson, R.G. DeVoe, S.H. Perlmutter, and D.F. Walls, Phys. Rev. Lett. **57**, 691 (1986).

[2] K. Bergman and H.A. Haus, Opt. Lett. **16**, 663 (1991).

[3] L.G. Joneckis, and J.H. Shapiro, *Quantum Electronics and Laser Science Conference*, Vol. 12 of 1993 Technical Digest Series (Optical Society of America, Washington, D.C., 1993), p. 282.

[4] L.J. Joneckis, J.H. Shapiro, J. Opt. Soc. B **10**, 1102 (1993).

[5] K.J. Blow, R. Loudon, and S.J.D. Phoenix, J. Opt. Soc. B **8**, 1750 (1991).

[6] G.P. Agrawal, *Nonlinear Fiber Optics* (Academic, New York, 1989).

[7] H.P. Yuen and J.H. Shapiro, IEEE Trans. Inform. Theory **IT-24**, 657 (1978).

[8] H.P. Yuen and J.H. Shapiro, IEEE Trans. Inform. Theory **IT-26**, 78 (1980).

[9] R.M. Shelby, (personal communication).

[10] C.W. Gardiner, *Handbook of Stochastic Methods for Physics, Chemistry and Natural Sciences* (Springer-Verlag, New York, 1985).

[11] S.J. Carter, P.D. Drummond, M.D. Reid, and R.M. Shelby, Phys. Rev. Lett. **58**, 1841 (1987).

[12] S.J. Carter, and P.D. Drummond, J. Opt. Soc. B **4**, 1565 (1987).

[13] Y. Lai, and H.A. Haus, Phys. Rev. A **40**, 844 (1989).

[14] Y. Lai, and H.A. Haus, Phys. Rev. A **40**, 854 (1989).

[15] P.D. Drummond, Phys. Rev. A **42**, 6845 (1990).

[16] S.J. Carter, P.D. Drummond, Phys. Rev. Lett. **67**, 3757 (1991).

[17] H.A. Haus, and F.X. Kärtner, Phys. Rev. A **46**, R1175 (1992).

[18] B. Yurke, Phys. Rev. A **35**, 3974 (1987).